



0017-9310(95)00092-5

Effect of mass transfer on turbulent friction during condensation inside ducts

W. GROENEWALD and D. G. KRÖGER†

Department of Mechanical Engineering, University of Stellenbosch, Stellenbosch, South Africa

(Received 18 January 1994 and in final form 16 February 1995)

Abstract—This paper quantifies the effect of mass transfer (suction) on wall friction for turbulent vapour flow inside ducts during condensation. Correlations are presented for the friction factor in terms of the suction rate, and are utilized in estimating the frictional pressure change in condenser tubes. These correlations are derived from the numerical integration of the velocity profile through the turbulent boundary layer, based on the Van Driest model for the Prandtl mixing length. Predictions of the frictional pressure drop during the condensation of steam in an air-cooled duct correspond to within $\pm 5\%$ of experimental measurements.

INTRODUCTION

Condensation inside ducts is an important process in the power and chemical industries. The design of an air-cooled condenser involves the sizing of the condenser to perform the required heat transfer duty with a minimum pressure drop during condensation. The estimation of the overall pressure change is hence of obvious relevance. The calculation of the pressure change is usually performed by integrating the local pressure gradient along the duct. Accurate modelling of the local pressure gradient is therefore required.

An abundance of literature exists (see, for example, Hewitt [1]) regarding the calculation of the pressure change in adiabatic two-phase flow systems. In situations where a change in phase is encountered, as during condensation, these adiabatic models yield inaccurate frictional pressure drop estimations since the frictional pressure drop is additionally influenced by a condensing mass flux towards the vapour-liquid interface. This mass flux alters the vapour velocity profile considerably in the vicinity of the interface and causes an increase in interfacial friction. This increase in interfacial friction is usually modelled [1, 2] by multiplying the adiabatic friction with a suitable enhancement factor β to account for the distortion of the vapour velocity profile. The friction enhancement factors that are traditionally used [2–4] stem from approximate theoretical analyses for turbulent flow over a porous flat plate [5–7] through which some of the fluid is sucked. These models give expressions for β in terms of a so-called ‘blowing’ parameter b_f , defined as $b_f = 2G_w/C_{f0}G_\infty$, where G_w is the mass flux at the wall surface and G_∞ is the free-stream mass flux, i.e. $G_\infty = v_\infty\rho_\infty$, and C_{f0} is the Fanning friction factor for the case of zero suction, i.e. $b_f = 0$. The model

presented in Mickley *et al.* [5] and Kays and Crawford [6] gives $\beta = C_f/C_{f0} = b_f/[\exp(b_f) - 1]$. Kays and Crawford [6] note that this expression is an excellent representation of experimental evidence for the no-pressure gradient case if C_{f0} is evaluated at the same x -Reynolds number, $Re_x = xv_\infty/\nu$, along the plate. However, since external flows differ from internal duct flows, some uncertainty exists as to the applicability of this expression to duct flows. Whereas external flows are characterized by an x -Reynolds number, $Re_x = xv_\infty/\nu$, duct flows are characterized by a Reynolds number based on the hydraulic diameter and mean velocity in the duct, $Re_g = d_h v_{xm}/\nu$. This difference results primarily from the fact that for external flows the boundary layer grows in thickness in the direction of flow, but in duct flows remains at a constant thickness that extends from the wall to the duct centre-line. The condition of equivalent x -Reynolds number has therefore no relevance in duct flows. Another complication associated with the blowing parameter b_f is that it is based on the free-stream velocity v_∞ . Since the turbulent velocity profile is relatively flat in duct flows, Blangetti *et al.* [3] recommended that v_∞ be substituted by the average duct velocity v_{xm} . An additional disadvantage of the ‘blowing’ parameter concept is that the friction enhancement factor is a complex function of C_f , thereby rendering the analytical integration of the friction along the flow direction impossible.

In view of these shortcomings prevalent in current frictional pressure drop modelling, approximate correlations for the friction enhancement factor β are derived for two duct geometries, namely channel and pipe flow. These correlations can easily be integrated analytically to obtain simple expressions for the frictional pressure drop in condenser tubes. These frictional pressure drop predictions are compared with experimental measurements obtained during the con-

† Author to whom correspondence should be addressed.

The turbulent eddy diffusivity may be modelled according to the Prandtl mixing length theory

$$\varepsilon_m = \iota^2 \left| \frac{\partial v_x}{\partial y} \right| \quad (8)$$

where the mixing length, ι , is proportional to the distance y from the wall in the logarithmic layer. The viscous sublayer immediately adjacent to the wall is generally modelled by introducing a damping function D that forces ι to zero at the wall [6, 10]:

$$\iota = \kappa y D. \quad (9)$$

Van Driest proposed an eddy diffusivity scheme [6] that allows the influence of the viscous sublayer to decay smoothly from the wall into the logarithmic layer

$$D = 1 - \exp(-y^+/A^+). \quad (10)$$

The constant A^+ represents an effective sublayer thickness with a value of approximately 26.0 for flow over a flat plate. Since transpiration and pressure gradient influence the effective sublayer thickness, the constant A^+ has been correlated to the Stanford experimental data for suction with negligible pressure gradient [6]

$$A^+ = \frac{26.0}{9.0v_{yw}^+ + 1.0} \quad \text{for } v_{yw}^+ < 0. \quad (11)$$

Substitute equations (7)–(10) into equation (6) to obtain after some manipulation an expression for the velocity gradient:

$$\frac{dv_x^+}{dy^+} = \frac{2F}{1 + \{1 + 4\kappa^2 y^{+2} F [1 - \exp(-y^+/A^+)]^2\}^{0.5}} \quad (12)$$

where $F = (1 + v_{yw}^+ v_x^+)$. The accuracy of integrating equation (12) numerically to obtain the velocity profile is ascertained by comparing the numerical results with experimental measurements of Rotta, taken for flow over a flat plate for various values of the suction parameter v_{yw}^+ [11]. Comparative results are shown in Fig. 1. The agreement is seen to be excellent.

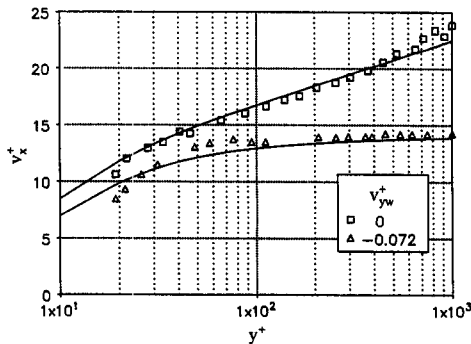


Fig. 1. Numerical solution indicating the effect of suction on the turbulent boundary layer velocity profile compared with the experimental data of Rotta (Ref. [12]) [11].

The deformation of the boundary layer due to suction is evident in the structural changes that take place within the boundary layer. From Fig. 1 it is seen that the sublayer and overlap layer have increased in thickness, with the logarithmic region progressively further from the wall with increasing suction.

Duct flow

Although the velocity profile resulting from the integration of equation (12) is derived for flow over a flat plate, it may also be extended to duct flows. The validity of this assumption is borne out by the fact that the logarithmic law of the wall is universally applicable and is essentially the same for duct and plate flows. The pressure gradient in duct flows appears to have a negligible influence on the velocity profile, except near the outer edge of the boundary layer where the wake region is considerably reduced. Since equation (6) is based on the Couette flow assumption, it is invalid near the outer edge of the boundary layer, i.e. near the centre-line of the duct. However, in duct flows the outer wake region is relatively small and velocity changes slight, and the velocity profile [as obtained from equation (12)] may be integrated across the duct cross-sectional area to obtain the average velocity in the duct [9].

Defining a suction Reynolds number, $Re_w = -v_{yw}d_h/v$, the dimensionless suction velocity v_{yw}^+ can be determined for various values of Re_w from $-v_{yw}^+ = Re_w/d_h$. The effective friction factor f_e for duct flows is defined as

$$f_e = \frac{8\tau_w}{\rho v_{xm}^2} = \frac{8v^{*2}}{v_{xm}^2} = \frac{8d_h^{+2}}{Re_g^2} \quad (13)$$

where the flow Reynolds number is given by $Re_{dh} = v_{xm}d_h/v$ and $d_h^+ = d_h v^*/v$.

In order to evaluate the friction factor at various suction rates, it is necessary to know the functional relationship $Re_{dh} = Re_{dh}(d_h^+)$ which depends on the tube geometry. Two different duct geometries, namely channel and pipe flow, are considered

Channel flow

For flow between two parallel plates separated by a distance $2h$, the hydraulic diameter d_h is equal to $4h$. The corresponding Reynolds number in terms of the wall coordinates is

$$Re_g = \frac{4hv_{xm}}{v} = 4 \int_0^{h^+} v_x^+ dy \quad (14)$$

where the velocity profile v_x^+ is obtained by integrating equation (12). The corresponding effective friction factor is given by equation (13) as

$$f_e = \frac{8d_h^{+2}}{Re_{dh}^2} = \frac{128h^{+2}}{Re_{dh}^2}. \quad (15)$$

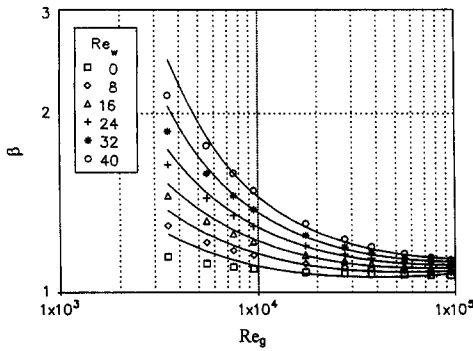


Fig. 2. Comparison between the correlation of β (solid line) and the numerical solution (symbols) for flow in a channel subjected to different suction rates.

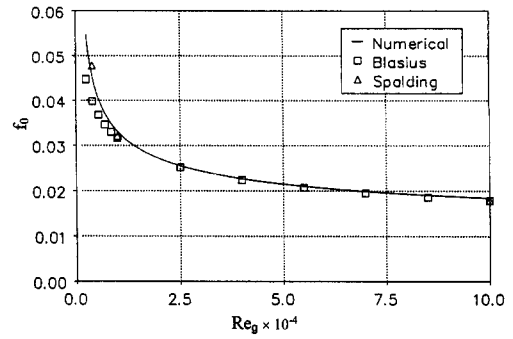


Fig. 3. Numerical solution for friction in a smooth tube compared with the Blasius equation and Spalding's law of the wall [9]

Performing the indicated integration in equation (14) with a fourth-order Runge–Kutta procedure and substituting the numerical results into equation (15) yields values of friction factor for various suction rates over a range of flow Reynolds numbers. Normalizing the resultant effective friction factor by the Blasius equation for smooth walls

$$f_0 = 0.3164 Re_g^{-0.25} \tag{16}$$

an approximate correlation for the friction factor at various suction rates is obtained for $3 \times 10^3 \leq Re_g \leq 1 \times 10^5$

$$\beta = \frac{f_e}{f_0} = C_1 + \frac{C_2}{Re_g} \tag{17}$$

where the constants C_1 and C_2 are functions of Re_w within the range $0 \leq Re_w \leq 40$

$$\begin{aligned} C_1 &= 1.0649 + 1.0411 \times 10^{-3} Re_w - 2.0110 \times 10^{-7} Re_w^3 \\ C_2 &= 290.1479 + 59.3153 Re_w + 1.5995 \times 10^{-2} Re_w^3. \end{aligned} \tag{18}$$

This correlation is presented graphically in Fig. 2 together with the exact values as determined from the numerical solution. The agreement is quite good, especially at high Re_g . From the figure it is seen that $\beta > 1$ for zero suction. This phenomenon is mainly attributable to: (i) the approximate nature of the Blasius equation which yields values that are slightly too low at Reynolds numbers near transition; (ii) inaccuracies induced by the hydraulic diameter concept [13]; and (iii) the extension of the Couette flow assumption to the complete boundary layer and thereby neglecting the slight wake region near the centre-line

Pipe flow

For flow in a pipe with radius a , the mean velocity is given in terms of the coordinate y , measured from the wall, $y = a - r$

$$\begin{aligned} v_{xm} &= \frac{1}{\pi a^2} \int_0^a 2\pi r v_x dr \\ &= \frac{2}{a} \int_0^a v_x dy - \frac{2}{a^2} \int_0^a v_x y dy. \end{aligned} \tag{19}$$

Introducing the wall coordinates $v_x^+ = v_x/v^*$ and $y^+ = yv^*/\nu$, the Reynolds number in the tube is obtained from

$$Re_g = \frac{v_{xm} d}{\nu} = 4 \int_0^{a^+} v_x^+ dy^+ - \frac{4}{a^+} \int_0^{a^+} v_x^+ y^+ dy^+. \tag{20}$$

Performing the indicated integration with a fourth-order Runge–Kutta procedure for various values of v_{yw}^+ yields the relationship $Re_g = Re_g(a^+)$ required to solve for the friction factor. From equation (13)

$$f_e = \frac{8d^{+2}}{Re_g^2} = \frac{16a^{+2}}{Re_g^2}. \tag{21}$$

The accuracy of this friction factor calculation is shown in Fig. 3, where the friction factor for zero suction is compared with the Blasius equation for smooth walls, equation (16), and also with results obtained from integrating Spalding's law of the wall [9]

$$\begin{aligned} y^+ &= v_x^+ + \exp(-\kappa B) \\ &\times \left[\exp(\kappa v_x^+) - 1 - \kappa v_x^+ - \frac{(\kappa v_x^+)^2}{2} - \frac{(\kappa v_x^+)^3}{6} \right] \end{aligned} \tag{22}$$

where the constants (κ ; B) are given by Nikuradse as (0.40; 5.5) [9].

The agreement between the present calculation and that of Spalding is quite good, confirming the validity of the approximations employed. The Blasius equation yields results that are conservative at low Reynolds numbers

Normalizing the effective friction factor calculation with the Blasius equation yields a correlation for β

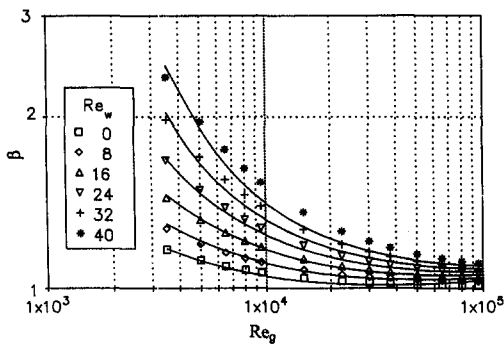


Fig. 4. Comparison between the correlation for β (solid line) and the numerical solution (symbols) for flow in a pipe subjected to different suction rates.

similar to equation (17), where the constants C_1 and C_2 are now given by

$$C_1 = 1.0046 + 1.719 \times 10^{-3} Re_w - 9.7746 \times 10^{-6} Re_w^2$$

$$C_2 = 74.3115 + 24.2891 Re_w + 1.8515 Re_w^2 \quad (23)$$

This correlation is shown in Fig. 4, together with the numerical calculation for various suction rates.

APPLICATION TO CONDENSING SYSTEMS

The condensation of a flowing vapour in a condenser tube causes a condensing flow towards the tube walls, which is in effect analogous to a suction flow in a duct with porous walls through which some of the fluid is sucked. This suction effect causes the interfacial friction to increase. In order to determine the overall frictional pressure drop, it is necessary to integrate the local frictional pressure gradient along the condensation path

$$\Delta p_f = - \int_0^L \frac{f_{ie} \rho_g}{2d_h} v_{gx}^2 dx \quad (24)$$

Since the local frictional pressure gradient is dependent on the local vapour velocity v_{gx} , it is important to know the vapour velocity distribution along the tube. In air-cooled condensing systems the major resistance to heat transfer lies on the air side [8], with the result that the heat flux remains approximately constant along the condenser tube. This condition causes the vapour velocity to decrease linearly from the tube inlet to the outlet:

$$v_{gx} = v_{gi} - (v_{gi} - v_{go}) \frac{x}{L} \quad (25)$$

Since the interfacial friction is generally a function of vapour Reynolds number, it is convenient to write equation (24) with the aid of equation (25) and the definition for Reynolds number in terms of local Reynolds number

$$\Delta p_f = \frac{\mu_g L}{2\rho_g Re_{gi} d_h^3} \int_{Re_{go}}^{Re_{gi}} f_{ie} Re_g^2 dRe_g \quad (26)$$

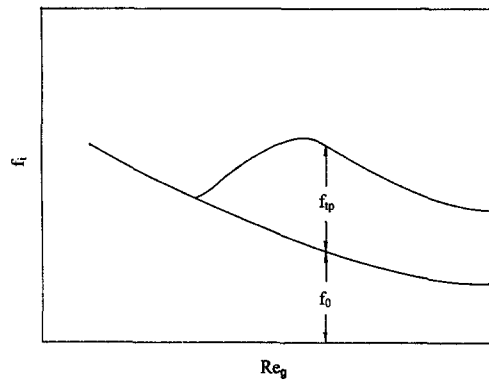


Fig. 5. Effect of wave formation on the two-phase friction factor in annular films [13].

In evaluating the integral in equation (26) it is necessary to know the functional relationship between the effective interfacial friction factor f_{ie} and the Reynolds number. In adiabatic two-phase flows, the friction factor normally exceeds that for single-phase flow if a certain minimum gas flow rate is exceeded for a given liquid flow rate [3]. This phenomenon is illustrated in Fig. 5 for annular flow, where the adiabatic interfacial friction factor f_i is shown to consist of two terms:

$$f_i = f_0 + f_{tp} \quad (27)$$

The term f_0 accounts for the friction within the entire gas boundary layer, and corresponds to the friction experienced in single-phase flow in a tube with smooth walls. The so-called two-phase component of friction f_{tp} represents the work done in the formation of waves in the liquid film, as well as the effect of separation of the gas boundary layer in the vicinity of the irregular gas-liquid interface.

In condensing flows, however, the friction is additionally influenced by the suction effect of the condensing vapour flow towards the interface. This effect influences only the single-phase portion of the total friction since the work required for wave formation remains unaltered [3]. Denoting this magnifying effect on the single-phase friction by the factor β , the effective friction factor in condensing flows is given by

$$f_{ie} = \beta f_0 + f_{tp} \quad (28)$$

In situations where the liquid film is relatively smooth, the adiabatic two-phase friction factor corresponds closely to the single-phase friction factor. The effective interfacial friction may then be modelled according to equations (16) and (17) for turbulent flow:

$$f_{ie} = \beta f_0 = 0.3164 \left[\frac{C_1}{Re_g^{0.25}} + \frac{C_2}{Re_g^{1.25}} \right] \quad (29)$$

Employing the definition for Reynolds number and substituting equations (25) and (29) into equation (26) yields, after integration,

$$\Delta p_f = \frac{0.3164 \mu_g^2 L}{2 \rho_g Re_{gi} d_h^3} \left[\frac{C_1}{2.75} (Re_{gi}^{2.75} - Re_{go}^{2.75}) + \frac{C_2}{1.75} (Re_{gi}^{1.75} - Re_{go}^{1.75}) \right] \quad (30)$$

The coefficients C_1 and C_2 are functions of suction Reynolds number, $Re_w = -d_h v_w / \nu$. For a constant heat flux Re_w is related to the inlet and outlet Reynolds numbers by

$$Re_w = \frac{d_h}{4L} (Re_{gi} - Re_{go}). \quad (31)$$

In the derivation of equation (30) it has been assumed implicitly that the vapour leaving the tube is still turbulent, i.e. $Re_{go} > 3000$. However, for complete condensation of an initially turbulent vapour, the flow reverts to a laminar nature at a certain transition Reynolds number. Although this transition is accelerated by the stabilizing effect of condensation, this effect is found to be negligible [8]. Transition may therefore be taken at the same value as for pipe flow, i.e. $Re_g = 2300$. In situations where the vapour inlet Reynolds numbers are relatively large ($Re_{gi} > 7500$), the laminar flow region is relatively short and it is found that equation (30) may be extrapolated to $Re_{go} = 0$, to include the laminar region, without any significant loss in accuracy [8] ($\Delta p_f < 1\%$ too high).

EXPERIMENTAL INVESTIGATION

The accuracy of the frictional pressure drop prediction is assessed experimentally for condensation of steam in an air-cooled flattened tube. A cross-section of the tube is shown in Fig. 6.

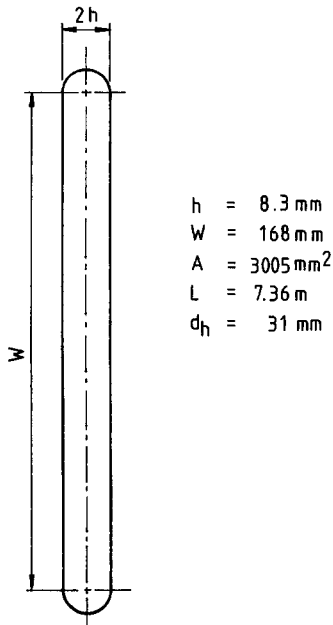


Fig. 6. Cross-sectional flow area of flattened tube.

A schematic diagram of the test facility is shown in Fig. 7. In order to simulate the behaviour of practical air-cooled condensers, a 7.36 m long fintube (3) installed at 60° to the horizontal was used. The tube consists of four 1.84 m sections, internally electro-galvanized to prevent corrosion, and mounted separately in a wooden air duct unit. Air is drawn from the surroundings via a bellmouth entrance and flows over the tube into the different airbox units. From each airbox the air flows through a balancing valve (8) to join the air from the other boxes. The air then flows to a 450 mm centrifugal fan (14) and is exhausted to the atmosphere via the laboratory window. Air can be bled into the fan by means of a butterfly regulating valve (13) to reduce the air flow over the tube. The air inlet temperatures are measured with 12 copper-constantan thermocouples installed along the length of the bellmouth inlet. Three thermocouples are located in each airbox in such a manner as to ensure an equal volume flow of air across each thermocouple. The existing air temperatures are likewise measured.

The separate fintube sections are flanged between stainless steel measuring discs, which are fitted with o-rings and temperature measuring points. At the bottom fintube section a steam exit box is fitted. A positive displacement pump (6) returns the cooled condensate from the subcooler to the evaporator (10). The steam temperatures along the tube are measured with sleeved copper-constantan thermocouples, installed two to a measuring disc which is sandwiched between the flanges of consecutive fintube sections.

The vacuum in the system is maintained by a simple venturi type vacuum pump (4), which is powered directly by line water. The vacuum pump is connected to the end of the fintube furthest removed from the steam inlet where non-condensables are likely to accumulate.

Hot water from an electric boiler is pumped to the evaporator (10) via large supply lines (15) to ensure high water flow rates and consequently high heat transfer rates. The evaporator water (on the shellside) is occasionally drained between tests via a drain pipe (16) to ensure water purity in the system. The steam generated in the evaporator flows through a supply pipe section (7) which is fitted for downflow tests with a pitot-static tube (17) to measure steam flow rates. This serves as a control check for the heat transfer calculations. The evaporator and steam supply tubing are covered with insulation material.

The fintubes (7), bellmouth air inlet and balancing valves (8) are all attached to a steel frame which has a swivel point at the floor. A catwalk at a height of 5 m (the laboratory is 8 m high) allows access to the top header box and safety devices to hold the apparatus.

The total pressure change across the condenser tube is measured with a differential pressure transducer. One side of the diaphragm is connected to the test tube outlet, while the other side is connected to the steam inlet header via an electrically heated and insulated copper tube. Due to this measuring arrange-

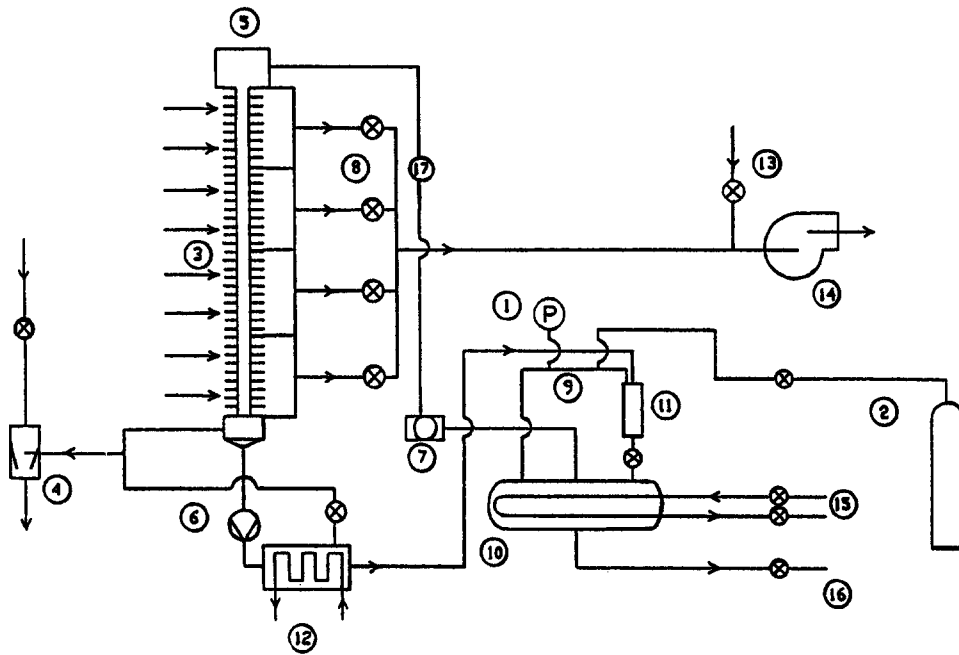


Fig. 7. Schematic diagram of the test facility.

ment, the total pressure change includes the pressure drop across the inlet header. This necessitated the accurate calibration of the inlet constant K_c . This was achieved by calibrating the inlet header pressure loss with air. The calibration was done for two different inlet configurations, i.e. rounded and sharp inlet flanges respectively, in order to make certain that fluid property effects were eliminated, since steam would be used in the practical application. A full description of the test facility and instrumentation is given in ref. [8]. The steam temperature was maintained at a constant value throughout a test by assuring that the system has attained a steady state condition. Different steam temperatures were realized by adjusting the electrical resistance of the heater elements in the boiler supplying water to the evaporator.

EXPERIMENTAL DATA AND EVALUATION

Experimental measurements of the total pressure change along the flat-profile condenser tube were recorded for saturation steam temperatures between 45 and 62°C. Various heat fluxes were attained, resulting in steam inlet Reynolds numbers ranging from 10 800 to 20 000. These ranges are representative of conditions experienced in practical air-cooled condenser applications. Since the total pressure change along the condenser tube is measured, this measurement includes the pressure drop resulting from the contraction in flow area from the inlet header to the tube, $\Delta p_i = (1 + K_c - \sigma^2)0.5\rho_g v_{gi}^2$, as well as the pressure gain caused by the deceleration of the vapour, $\Delta p_m = -\alpha_m \rho_g (v_{gi}^2 - v_{go}^2)$, and the change in elevation from the tube inlet to outlet, $\Delta p_g = \rho_g g L \sin 60^\circ$. For turbulent

flow the momentum correction factor is taken as $\alpha_m \approx 1$ [14], and the ratio of the tube to header area $\sigma = 0.186$. The inlet constant K_c was precalibrated with air flow for both the rounded ($K_c = 0.21$) and sharp ($K_c = 0.60$) inlet flanges.

In the range of heat fluxes covered in the experiment, the liquid film was relatively smooth and the adiabatic two-phase friction factor f_i was found to correspond closely to the single-phase value f_0 [12], thereby validating the use of equation (30) in the prediction of the frictional pressure drop. Due to the high aspect ratio of the tube (height : width = 11 : 1), the vapour flow may be approximated by channel flow. This approximation enables the use of equation (18) for the calculation of the constants C_1 and C_2 in equation (30).

A comparison between the theoretical and experimental frictional pressure drop data is shown in Fig.

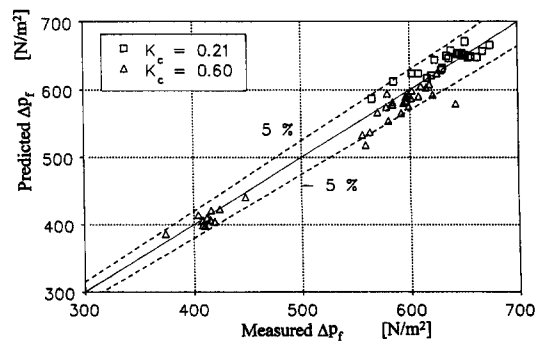


Fig. 8. Comparison between experimental and predicted frictional pressure drop.

8. The agreement is seen to be within $\pm 5\%$ in the range of steam inlet Reynolds numbers and temperatures covered. The model is seen to have a slight tendency to overpredict, which is the result of extending the expression for the turbulent friction to include the laminar region as well.

Acknowledgements—The financial support of the South African Water Research Commission and The Foundation for Research and Development is gratefully acknowledged.

REFERENCES

1. G. F. Hewitt, Pressure drop and void fraction. In *Handbook of Multiphase Systems* (Edited by G. Hetsroni), Chap. 2. McGraw-Hill, New York (1982).
2. R. G. Sardesai, R. G. Owen and D. J. Pulling, Pressure drop for condensation of a pure vapour in downflow in a vertical tube, *Proceedings of the Seventh Heat Transfer Conference*, pp. 139–145. München (1982).
3. F. Blangetti, R. Krebs and E. U. Schlünder, Condensation in vertical tubes—experimental results and modelling, *Chem. Engng Fundam.* **1**, 20–63 (1982).
4. V. G. Rifert, Heat transfer and flow modes of phases in laminar film vapour condensation inside a horizontal tube, *Int. J. Heat Mass Transfer* **31**, 517–523 (1988).
5. H. A. Mickley, R. C. Ross, A. L. Squyers and A. L. Stewart, Heat, mass and momentum transfer to flow over a flat plate with blowing or suction, NACA TN 3208 (1954).
6. W. M. Kays and M. E. Crawford, *Convective Heat and Mass Transfer* (2nd Edn), Chap. 10. McGraw-Hill, New York (1980).
7. S. S. Kutateladze and A. I. Leont'ev, *Turbulent Boundary Layers in Compressible Gases* (1st Edn), Chap. 2. Edward Arnold, London (1964).
8. W. Groenewald, Heat transfer and pressure change in an air-cooled flattened tube during condensation of steam, M.Eng. Thesis, University of Stellenbosch, Stellenbosch, South Africa (1994).
9. F. M. White, *Viscous Fluid Flow* (2nd Edn), Chap. 6. McGraw-Hill, New York (1991).
10. W. M. Kays, Heat transfer to the transpired turbulent boundary layer, *Int. J. Heat Mass Transfer* **15**, 1023–1044 (1972).
11. H. Schlichting, *Boundary Layer Theory* (7th Edn), p. 647. McGraw-Hill, New York (1979).
12. J. C. Rotta, Control of turbulent boundary layers by uniform injection or suction of fluid. *Jb 1970 Dt. Gesellschaft für Luft- und Raumfahrt*. (Edited by H. Blenk and W. Schulz), pp. 91–104. Braunschweig (1971).
13. R. C. Funnell, Personal communication, Department of Mechanical Engineering, University of Stellenbosch, South Africa (1991).
14. W. M. Kays, Loss coefficients for abrupt changes in flow cross section with low Reynolds number flow in single and multiple-tube systems, *Trans. ASME* **72**, 1067–1074 (1950).